

PDF hosted at the Radboud Repository of the Radboud University Nijmegen

The following full text is a publisher's version.

For additional information about this publication click this link.

<http://hdl.handle.net/2066/112838>

Please be advised that this information was generated on 2017-12-06 and may be subject to change.

Carrier-concentration-dependent electron-LO-phonon coupling observed in GaAs-(Ga,Al)As heterojunctions by resonant-polaron cyclotron resonance

C. J. G. M. Langerak, J. Singleton, P. J. van der Wel, and J. A. A. J. Perenboom

High Field Magnet Laboratory and Research Institute for Materials, University of Nijmegen, Toernooiveld, NL-6525 ED Nijmegen, The Netherlands

D. J. Barnes, R. J. Nicholas, and M. A. Hopkins*

The Clarendon Laboratory, Parks Road, Oxford OX1 3PU, United Kingdom

C. T. B. Foxon

Philips Research Laboratories, Redhill RH1 5HA, United Kingdom

(Received 15 July 1988)

The cyclotron resonance (CR) of the two-dimensional electron gas (2D EG) in GaAs-(Ga,Al)As heterojunctions has been studied in the resonant-polaron regime for 2D carrier densities N_s in the range $(0.8-5.4) \times 10^{11} \text{ cm}^{-2}$. A reflectivity technique has allowed the CR to be recorded at energies up to 35.63 meV, within the GaAs reststrahlen band, and a calculation of the dielectric response of the complete heterostructure has enabled the effective masses to be reliably evaluated from the line shapes and positions of the resonances. The results indicate that the 2D electrons are coupling to the LO phonon (36.7 meV), in agreement with theoretical predictions. At low carrier densities, the resonant-polaron contribution to the effective mass becomes apparent at cyclotron energies above 25 meV, and increases in size as the LO-phonon energy is approached: however, this mass enhancement is removed rapidly as N_s is increased, indicating the importance of Landau-level occupancy and screening in the 2D EG. Close to the LO-phonon energy, large shifts in the resonance position, which are several times the linewidth in size, are produced by varying N_s . This large N_s dependence explains previous conflicting reports of "enhanced" or "reduced" polaron effects in the 2D electron gas. A comparison of the experimental results with existing memory-function calculations of the polaron contribution to the effective mass indicates that the greater part of the N_s dependence can be ascribed to Landau-level occupancy effects.

I. INTRODUCTION

The interaction of a two-dimensional electron gas (2D EG) with optic phonons in polar semiconductor systems has been the subject of a great number of theoretical and experimental studies. In equivalent experimental studies of bulk (3D) semiconductor systems¹⁻³ the electron density has usually been small ($\sim 10^{13} \text{ cm}^{-3}$ in GaAs), so that the electrons satisfy Boltzmann statistics: the polaron effects are well described by one-polaron theories.^{2,3} However, in most 2D systems, such as GaAs-(Ga,Al)As heterojunctions, the electron density is typically $\sim 10^{11} \text{ cm}^{-2}$, corresponding to a 3D electron density of $\sim 10^{17} \text{ cm}^{-3}$, and one-polaron theories are not necessarily valid. Initial theoretical work⁴⁻⁶ on the 2D EG was based on one-polaron approximations, and predicted an enhancement of the polaron effects over those in corresponding bulk systems, due to the relaxation of the need for wave-vector conservation in one direction. The available experimental data indicated 2D-polaron effects which were both reduced,⁷⁻¹¹ comparable¹² and enhanced^{8,13} with respect to those in bulk systems, and so subsequent theoretical approaches have included the finite extension of the electron wave function perpendicular to the 2D EG (Refs. 14 and 15) and many-particle effects, such as dynamical screening and the Landau-level occupation

effect arising from the Fermi-Dirac statistics.¹⁶ Both of these effects tend to reduce the coupling strength, and the theories have been fairly successful in describing the energy dependence of the cyclotron effective mass in GaAs-(Ga,Al)As heterojunctions at low temperatures and in magnetic fields up to 20 T. (Ref. 16) At higher temperatures the effective mass was found to increase,¹⁷ and this was ascribed to an increase in the polaron contribution to the effective mass. This variation in the polaron effect has been attributed to temperature-dependent screening,¹⁷ polaron nonparabolicity,^{18,19} or possibly the transition to nondegenerate statistics. Generally, in most of the above work, it has been assumed that the electrons in the 2D EG couple to longitudinal-optical (LO) phonons, as in bulk semiconductors. However, recently, both cyclotron-resonance²⁰ (CR) and magnetophonon-resonance¹⁷ (MPR) experiments performed on a variety of semiconductor heterojunctions have indicated apparent weak coupling of 2D electrons to a phonon of lower frequency, closer to the transverse-optical (TO) phonon. On the other hand, cyclotron-resonance results on lower-carrier-density quantum wells²¹ showed stronger coupling close to the LO-phonon frequency. The former results are very surprising, and if true, have implications for heterojunction devices working at room temperature, where the dominant scattering of electrons

is due to optical phonons. In this paper we have used cyclotron-resonance measurements on the well-characterized GaAs-(Ga,Al)As heterojunction system, to check to which optical phonon the electrons are coupling, and to assess the importance of screening and occupation effects, in order to explain some of the above-mentioned conflicting experimental data.

The energy spectrum of an electron in a magnetic field becomes quantized into Landau levels, and these are modified by the polaron effect in the following ways: (i) they are shifted to lower energy; (ii) the slopes of the Landau-level energies versus magnetic field are changed because of the mass renormalization of the electron; (iii) the Landau levels do not cross the virtual energy level formed by the lowest Landau level plus one optical phonon, because of von Neumann's anticrossing principle; and (iv) the Landau levels are pinned to the energy of that virtual level in high magnetic fields.^{22,23} In a cyclotron-resonance experiment, the separation of adjacent Landau levels, $\hbar\omega_c$, is measured as a function of magnetic field B , allowing the effective mass m^* to be deduced from the relationship $m^* = eB/\omega_c$. Due to the modifications to the Landau levels described above, at cyclotron energies below the optical-phonon energy, the measured effective mass will be greater than the band-structure mass, and increase due to the resonant-polaron interaction (i.e., the level anticrossing) as the optical-phonon energy is approached; after traversing the optical-phonon energy (the resonant-polaron condition), an effective mass smaller than the band-structure mass will be observed.²³ The cyclotron energy at which this discontinuity occurs is thus a very good indication as to the phonon to which the electrons are coupling, and the size of the discontinuity provides a measure of the strength of the interaction, enabling the influence of carrier density, etc., to be probed.²³

A problem with this technique when applied to GaAs-(Ga,Al)As heterojunctions occurs between the GaAs TO and LO frequencies, where there is virtually no far-infrared (FIR) transmission through the GaAs substrates on which most high-quality heterojunctions are grown. This makes it impossible to observe the resonant-polaron effect in the usual transmission configuration adopted for cyclotron resonance. We have circumvented this difficulty by studying the cyclotron resonance in a variety of GaAs-(Ga,Al)As heterojunctions using FIR *reflectivity* at energies very close to the GaAs LO-phonon frequency. These measurements indicate that the dominant interaction of 2D electrons in a heterojunction is in fact at the GaAs LO-phonon frequency, as in bulk semiconductors. The strength of the resonant-polaron effect has been

found to decrease dramatically with increasing 2D carrier density, illustrating the importance of occupation effects and screening. In Sec. II the details of the samples and measurement techniques are summarized. In Sec. III model calculations of the dielectric response of a heterojunction are presented: these are used to reliably extract the effective masses of the electrons from the reflectivity data. The results are discussed in Sec. IV, with particular reference to the electron-density dependence of the polaron effect, and compared with numerical calculations.

II. EXPERIMENTAL DETAILS

The GaAs-Ga_{1-x}Al_xAs heterojunctions used in the experiments were grown by means of molecular-beam epitaxy at Philips Research Laboratories;²⁴ sample details are shown in Table I. The samples had 2D areal electron densities (N_s) ranging from 0.8×10^{11} to $3.4 \times 10^{11} \text{ cm}^{-2}$ in the dark; N_s values up to $5.4 \times 10^{11} \text{ cm}^{-2}$ were achieved by illumination with a red light-emitting diode (LED). The electron concentration was determined in each case from low-field Shubnikov-de Haas oscillations. FIR radiation at frequencies close to the GaAs reststrahlen band was provided by a specially adapted optically pumped laser,²⁵ and the high magnetic fields necessary for the resonant-polaron condition were provided by a 25-T hybrid magnet or 20-T Bitter coil. The sample under study was placed at the magnet field center, with its upper surface 1 mm below a conical light guide from which the FIR radiation emerged; the diameter of the exit orifice of the cone was 1.5 mm. The substrate of the sample was wedged in order to prevent multiple reflections within the sample and a consequent distortion of the resonance line shape.²⁶ Great care was taken to position the sample so that the 2D EG was exactly perpendicular to the magnetic field, in order to avoid the modifications to the line shape and resonance position caused by resonant electric-subband-Landau-level coupling due to small in-plane magnetic fields.^{27,28} A carbon bolometer was placed above the sample just to one side of the cone, in order to detect the reflected radiation. The top layers of the samples are a few hundred angstroms thick, so that in reflectivity the FIR has only to traverse this distance twice, instead of the 200- μm -thick substrate in transmission. Similar bolometers were placed below the sample and in the light guide above the cone, in order to monitor the transmitted and incident FIR radiation, respectively, so that normalized transmission and reflection spectra could be simultaneously recorded. The sample and bolometers were immersed in helium exchange gas at a temperature of $T \approx 1.3 \text{ K}$.

TABLE I. Characteristics of the samples used in this study.

Sample	Cap layer GaAs (Å)	Doped (Ga,Al)As (Å)	N_d (cm^{-3})	Spacer (Ga,Al)As (Å)	x (Al fraction)	N_s (cm^{-2}) (dark)	μ ($\text{cm}^2 \text{V}^{-1} \text{s}^{-1}$) (dark)	N_s (cm^{-2}) (light)	μ ($\text{cm}^2 \text{V}^{-1} \text{s}^{-1}$) (light)
1	200	500	1.38×10^{18}	800	0.33	0.7×10^{11}	1.0×10^6	1.9×10^{11}	1.8×10^6
2	170	400	1.30×10^{18}	400	0.32	1.4×10^{11}	2.0×10^4	3.4×10^{11}	1.2×10^6
3	200	400	1.33×10^{18}	200	0.33	3.4×10^{11}	8.8×10^{15}	5.4×10^{11}	1.3×10^6

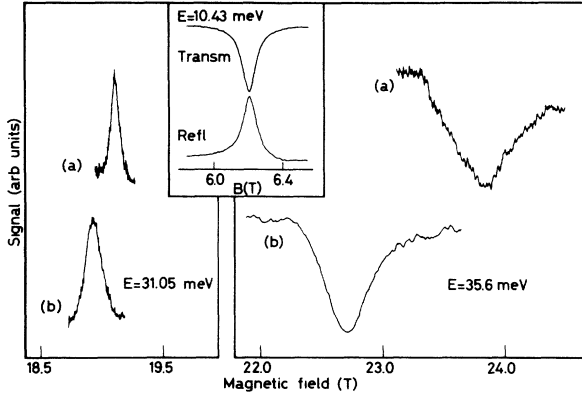


FIG. 1. Normalized reflectivity for GaAs-(Ga,Al)As heterojunction 3 at two different cyclotron energies, 31.05 and 35.63 meV, below and within the reststrahlen band, respectively. Data are shown for two carrier densities (a) $N_s = 3.4 \times 10^{11} \text{ cm}^{-2}$ and (b) $5.4 \times 10^{11} \text{ cm}^{-2}$, obtained by illumination with a red light-emitting diode: note how the resonance shifts to lower fields as N_s increases. The inset shows simultaneously recorded reflection and transmission traces, showing that outside the reststrahlen band, the reflectivity peak corresponds to the transmission minimum.

Figure 1 shows typical normalized reflectivity data for two different values of the 2D carrier density. At photon energies outside the reststrahlen band, the CR is observed as a peak in reflection,⁹ except at very low carrier densities. However, within the reststrahlen band, the CR appears as a minimum in reflectivity. Qualitatively, the latter result is due to the superposition of cyclotron absorption upon the very high reflectivity of the GaAs substrate; at the resonance field radiation is absorbed by the 2D EG before and after reflection from the GaAs, so that the reflected radiation is diminished. Note that in both cases the CR for the higher carrier density occurs at significantly lower magnetic fields, indicating a lower effective mass. This shift to lower field is much larger within the reststrahlen band (i.e., closer to the LO-phonon energy), and this is a visible manifestation of the suppression of the resonant-polaron effect due to the increasing carrier density, which will be discussed below. The inset of Fig. 1 shows the CR in reflectivity and transmission, and demonstrates that, outside the reststrahlen band, the peak in reflectivity corresponds to the minimum in transmission.⁹

III. DIELECTRIC RESPONSE OF A HETEROJUNCTION

The first reports of apparent weak resonant-polaron effects at the TO-phonon frequency were made as a result of transmission measurements on high-carrier-density (Ga,In)As heterojunctions grown on InP;^{20,21} the apparent very weak coupling was observed as a small discontinuity in the position of the minimum in transmission. Recently, Karraï *et al.*²⁹ have made a careful calculation of the dielectric response of such a heterojunction, and have shown that these apparent resonant-polaron effects and the observed cyclotron-resonance line

shapes can be explained as merely a consequence of the rapidly varying refractive indices of the component semiconductors; no polaron effects were necessary to reproduce the experimental results.

The work of Karraï *et al.*²⁹ illustrates the danger of simply associating the transmission minimum with the resonance position, close to the reststrahlen band. In order to evaluate the effective mass correctly from results such as the ones shown in Fig. 1, it is therefore necessary to calculate the full dielectric response of the heterostructure. For this purpose the sample is considered as three sections, a (Ga,Al)As top layer, followed by the 2D EG, which is assumed to reside within a thin layer of thickness d ($\sim 250 \text{ \AA}$) of GaAs, and finally the GaAs buffer layer and substrate, a few tenths of a millimeter thick. It was found that the exact thickness chosen for the layer containing the 2D EG made little difference to the results; the thicknesses of the other layers are taken from the sample growth data (Table I). The dielectric responses of the GaAs and the (Ga,Al)As are described using a classical single-mode damped-harmonic-oscillator model,

$$\epsilon(\omega) = \epsilon_\infty + \frac{\epsilon_\infty(\omega_{\text{LO}}^2 - \omega_{\text{TO}}^2)}{\omega_{\text{TO}}^2 - \omega^2 - i\gamma\omega}, \quad (1)$$

where ω_{TO} is the frequency of the TO phonon, ϵ_∞ is the high-frequency dielectric constant, and γ is a damping parameter. In the case of (Ga,Al)As this expression represents an approximation, as another "AlAs-like" set of optical phonons exist at much higher energies; however, these appear to make little difference to the calculated response close to the GaAs reststrahlen band, and so were omitted for simplicity. The phonon energies and damping parameters used in these expressions are shown in Table II and were obtained from the literature.³⁰ The classical 3D Drude form of the conductivity in a magnetic field is used to treat the 2D EG (Ref. 31),

$$\sigma(\omega) = \frac{n_s e^2}{m^*} \frac{1/\tau + i(\omega \pm \omega_c)}{1/\tau^2 + (\omega \pm \omega_c)^2}, \quad (2)$$

where $\omega_c = eB/m^*$ is the cyclotron frequency, n_s is the equivalent 3D electron concentration of the 2D EG (N_s/d), and τ is a relaxation time related to, but not in general equal to, that given by the dc mobility.³² Subsequently, the dielectric response of the 2D EG is given by

$$\epsilon(\omega) = \epsilon_{\text{GaAs}}(\omega) + \frac{i\sigma(\omega)}{\omega\epsilon_0}. \quad (3)$$

Alternatively, the interaction of the FIR radiation with the 2D EG can be modeled by deriving the Drude polarizability of an infinitely thin 2D EG.³³⁻³⁷ The latter ap-

TABLE II. Parameters used to represent the dielectric response of GaAs-(Ga,Al)As heterojunctions.

	ϵ_∞	γ (meV)	ω_{LO} (meV)	ω_{TO} (meV)
GaAs	10.9	0.31	36.7	33.9
(Ga,Al)As	10.9	0.31	35.0	33.4

proach and Eq. (3) both yield identical results, as the thickness of the 2D EG represents a length much shorter than the FIR wavelength. Note that the Drude conductivity, given by Eq. (2), or the Drude polarizability of Ref. 33 do not take any account of Fermi-Dirac statistics and occupation effects, and thus can only be used to represent the response of the 2D EG accurately when the system is in either the high-density limit (large Landau-level occupation number) or the quantum limit (at high magnetic fields where the occupancy is less than 2). At intermediate field strengths the oscillating level occupancies and transition matrix elements may lead to differences from the Drude predictions. The Drude formalism can lead to overestimates of the CR linewidth in the intermediate regime.³⁸

The total dielectric response of the heterojunction is then found by solving the continuity equations for the electric and magnetic fields of the photon at all interfaces: vacuum-(Ga,Al)As, (Ga,Al)As-2D EG, 2D EG-GaAs, and GaAs-vacuum. This is totally analogous to the transfer-matrix method.^{29,39} The wedging of the sample substrate was simulated by averaging calculations for many different substrate thicknesses.

In order to illustrate the regions in which a full simulation of the heterojunction dielectric response is necessary, we have calculated the position of the extremum in reflectivity (peak outside reststrahlen band, minimum inside) as a function of energy in the absence of resonant-polaron effects. The energy dependence of the cyclotron effective mass due to band nonparabolicity was described by the following expression:^{10,12,40}

$$\frac{1}{m^*(E)} = \frac{1}{m^*(0)} \left[1 + \frac{2\kappa_2 E}{E_g} \right]. \quad (4)$$

This relation has been found to represent existing data well and is a simplified version of Eq. (5), discussed below. E_g is the gap at the Γ point; the parameter κ_2 is known both from low-energy cyclotron-resonance measurements^{3,10,41,42} and recent 14-band theoretical treatments of GaAs,^{41,43} and its value is close to $\kappa_2 = -1.4$. The “zero-energy” effective mass $m^*(0)$ is chosen to be $0.0672m_e$, in order to fit the lower-energy results well; this enhancement over the bulk band-edge effective mass is due to confinement¹⁰ and some renormalization due to the nonresonant part of the polaron effect.^{4-6,12,14-16,22,23} A (Ga,Al)As top-layer thickness of 600 Å, a 2D EG thickness of 250 Å, and a 2D carrier density of $3.4 \times 10^{11} \text{ cm}^{-2}$ were assumed. Figure 2 shows the results of the calculation; the effective mass which would be derived by assuming that the reflectivity extremum represented the resonance position has been plotted as a function of energy. At energies outside the reststrahlen band, the extremum in reflectivity occurs at a magnetic field very close to the true resonance position. However, on passing through the optical-phonon energies, the extremum moves discontinuously, and within the reststrahlen band deviates from the resonance-field position. The largest deviation occurs just below the LO-phonon energy. Note that the discontinuities and deviations would be different if the transmission minimum

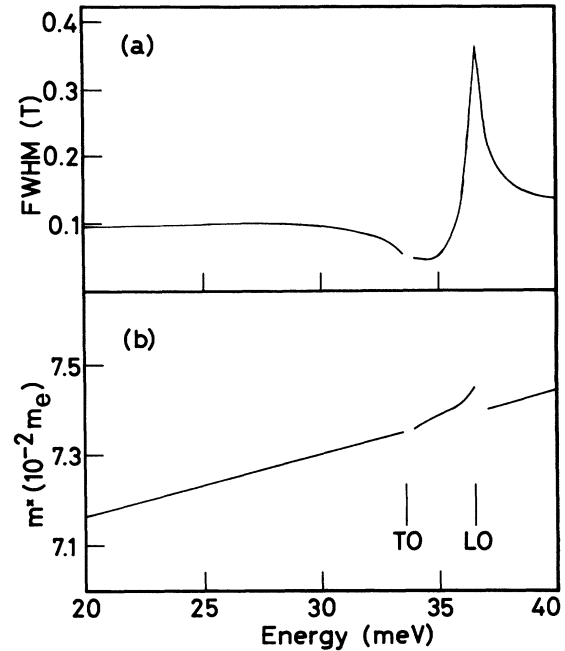


FIG. 2. (a) The cyclotron-resonance linewidth (FWHM) and (b) the effective mass m^* derived from the reflectivity extremum position as a function of energy in the absence of the resonant-polaron effects, calculated using the dielectric response model described in the text. The vertical lines indicate the phonon energies: between the phonons the reflectivity shows a minimum near resonance, whereas the response is a peak outside this region.

positions were plotted instead of the reflectivity extremum positions.²⁹ In addition, the full width at half maximum (FWHM) of the resonance in reflectivity predicted by the model has been plotted in Fig. 2; as τ is kept constant at 10.6 ps in the calculation, the increase in linewidth close to the LO-phonon energy shown here is due solely to dielectric effects.

Such calculations dictated the procedure for analyzing the experimental results. At energies far away from the reststrahlen band the experimental maximum in the

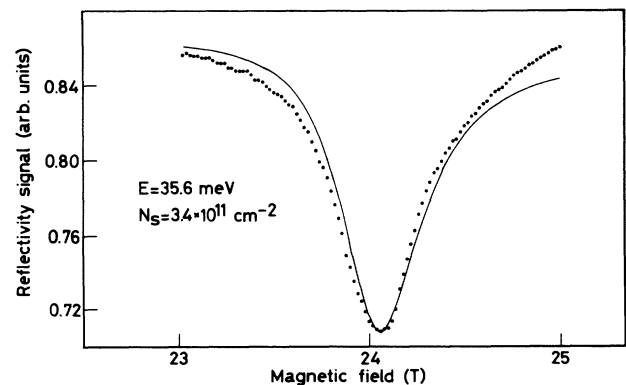


FIG. 3. Calculated reflectivity signal (solid line) compared to experimental data (points) for a cyclotron energy of 35.63 meV and a carrier density $3.4 \times 10^{11} \text{ cm}^{-2}$. The fitting parameters used were $m^* = 0.07787m_e$ and $\tau = 1.99 \text{ ps}$.

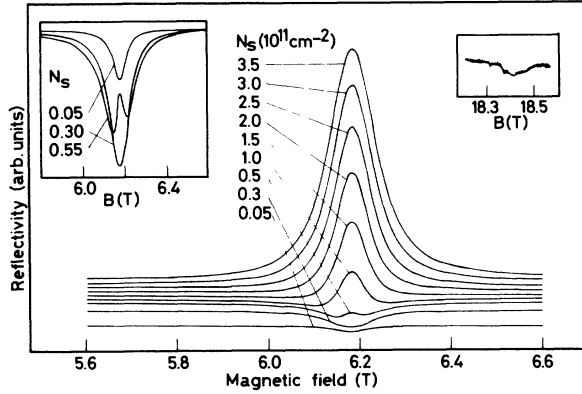


FIG. 4. A set of results from model calculations at 10.43 meV for several values of N_s : the predicted reflectivity signal shows a dip at the resonance position at low carrier densities, but a peak at high carrier densities. The traces for each density have been vertically displaced for clarity. The left-hand side inset in the figure is an expansion of the resonance close to the transition from peak to dip, while the right-hand side inset shows the experimental cyclotron resonance in reflectivity at 31.05 meV for a heterojunction with $N_s = 0.3 \times 10^{11} \text{ cm}^{-2}$; as predicted, the resonance is seen as a dip (compare Fig. 1).

reflectivity was taken as the exact resonance position, whereas close to and within the reststrahlen band the model for the dielectric response of the heterojunction was used to extract the cyclotron effective mass from the experimental reflection and transmission data: the (Ga,Al)As layer thickness was taken from the growth data (Table I) for each sample, and then the effective mass m^* and the scattering time τ were varied. It should be noted that all of the samples have carrier densities such that the electrons are all in the lowest Landau level at fields well below those corresponding to the reststrahlen band energies, and so Drude-like expressions for the conductivity of the 2D EG are expected to represent its response reasonably.³⁸ The model reproduces the line shape well (Fig. 3 shows a typical result), indicating that this is a reliable method of extracting the effective mass and scattering time of the electrons.

Before proceeding to the experimental results, it is useful to briefly examine further some of the general features of the simulated reflectivity data. Figure 4 shows a set of results of the model calculations for a FIR-radiation energy of 10.43 meV and for several values of the 2D electron concentration: an effective mass of $0.0674m_e$ and a scattering time of 10.6 ps have been assumed. The superposition of all the dielectric responses results, in general, in a peak in the region below the reststrahlen band. At low carrier densities, however, the CR is seen as a dip, which is most pronounced at $N_s = 0.3 \times 10^{11} \text{ cm}^{-2}$. The inset of this figure shows the reflectivity of a heterojunction with very low carrier density, showing that the reflective response is indeed a dip in this regime.

IV. DISCUSSION

The effective masses deduced from the experimental data as described above are shown as a function of cyclo-

tron energy in Fig. 5 for a variety of different carrier densities. Also shown for comparison are some data from bulk GaAs.^{3,7,42,44} The heterojunction effective masses show a gentle background increase as a function of energy, due to the band nonparabolicity,¹⁰ upon which the resonant-polaron contribution to the effective mass is superimposed. At low carrier densities and at cyclotron energies above 25 meV, the effective mass increases much faster with energy than expected from the band nonparabolicity alone: this is due to the resonant-polaron effect. As a consequence of this rapid increase in effective mass and the resonant increase in CR linewidth (see below),

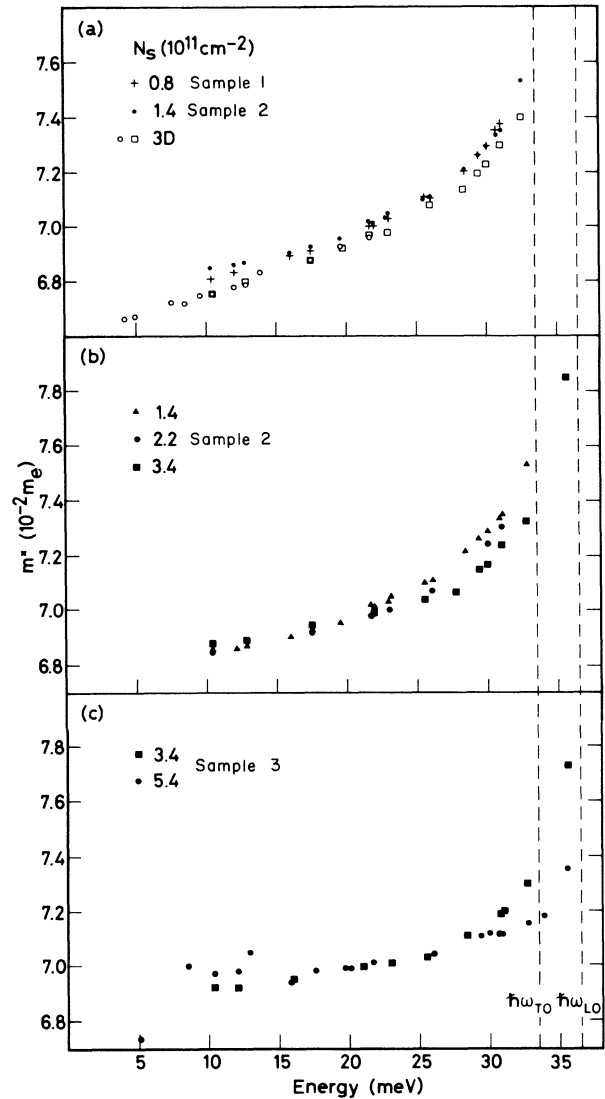


FIG. 5. The effective mass obtained from the measurements vs energy for the three samples (1–3) at several 2D electron concentrations (N_s). The data for sample 2 with $N_s = 1.4 \times 10^{11} \text{ cm}^{-2}$ are plotted in both (a) and (b) for ease of comparison. The TO- and LO-phonon energies are shown as vertical dashed lines. In (a) data from bulk GaAs are shown for comparison (\circ , Refs. 3 and 44; \square , Refs. 7, 42, and 44—these masses are the averages of the spin-up and spin-down cyclotron resonances for the [100] and [110] directions).

CR could not be observed within the reststrahlen band for these low carrier densities with the magnetic field strengths available. On increasing the 2D carrier density, the mass enhancement due to the resonant polaron effect is reduced; e.g., in sample 2 at $N_s = 3.4 \times 10^{11} \text{ cm}^{-2}$, the CR at an energy of 35.63 meV was observed at 24.16 T. This point lies close in energy to the LO phonon, and represents a mass enhancement of around 10% over the value expected from band nonparabolicity alone (see below). As the effective mass still appears to be increasing at this energy, coupling to the LO phonon is indicated. On further increasing the carrier density, using sample 3, the CR magnetic field at an energy of 35.63 meV falls from 23.79 T at $N_s = 3.45 \times 10^{11} \text{ cm}^{-2}$ to 22.64 T at $N_s = 5.42 \times 10^{11} \text{ cm}^{-2}$, a shift which is several times larger than the resonance linewidth (see Fig. 1). The latter field represents a mass enhancement of less than 3% over the value calculated from band nonparabolicity alone. It can be seen from Fig. 5 that for $N_s = 5.4 \times 10^{11} \text{ cm}^{-2}$, the resonant-polaron contribution to the effective mass is much reduced: however, data points just below and above the TO-phonon energy show a smooth increase in effective mass, continuing as the LO-phonon energy is approached. Thus, there is no indication of TO-phonon coupling, even at these high carrier densities. Note that at this carrier density the low-energy effective mass oscillates due to filling-factor effects.^{36,37,45}

It seems, therefore, that the cyclotron resonance indicates a resonant-polaron effect at the LO-phonon frequency, and hence, electron-LO-phonon coupling, in contrast to the magnetophonon results which indicated coupling to a phonon intermediate between the TO- and LO-phonon energies.^{17,46} In addition, the electron-phonon coupling strength appears to be dramatically reduced as the 2D carrier concentration is increased. We show this more explicitly in Fig. 6, where the effective mass at five different cyclotron energies is plotted as a function of the 2D electron concentration. For each energy, Fig. 6 shows a decrease of the effective mass as N_s is increased. The size of this decrease becomes progressively larger as the energy approaches the LO-phonon energy. This is a manifestation of the reduction in the resonant-polaron contribution to the effective mass.

The true strength of the polaron effect is somewhat masked by other factors depending on either N_s (e.g., subband confinement energy) or energy (band nonparabolicity). It is thus necessary to remove these band-structure-dependent factors from the data for a valid assessment of the polaron effect. This is also desirable if a comparison of data and theory is to be made, as all theoretical treatments derive the cyclotron mass with respect to the band-structure effective mass, a quantity which cannot be measured directly.⁴⁷ In order to represent the dependence of the effective mass on N_s and energy in the absence of polaron effects, the following expression, valid for electron energies much less than the band gap of GaAs, is used,⁴⁸

$$\frac{1}{m_b^*(E)} = \frac{1}{m_0^*} \left[1 + \frac{2\kappa_2}{E_g} (E + \langle T \rangle_z) \right], \quad (5)$$

where m_0^* is the bulk GaAs band-edge effective mass,

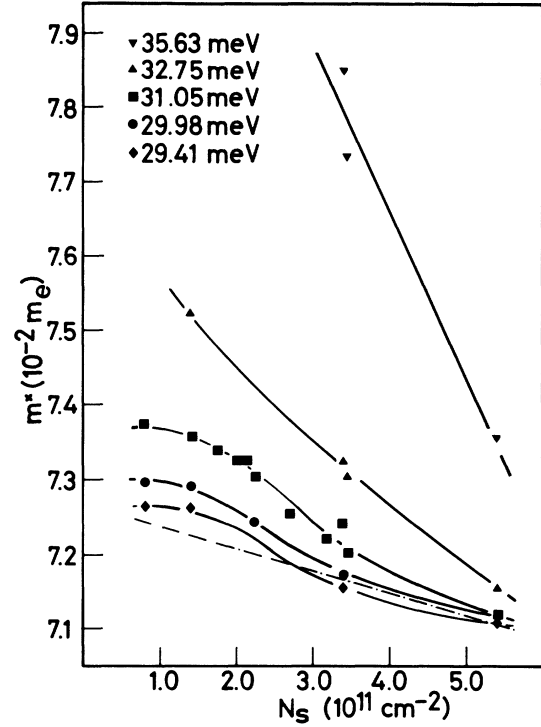


FIG. 6. The effective masses at several cyclotron energies as a function of the 2D electron concentration. Experimental data are shown as points; the solid lines are guides to the eye. The dashed-dotted line shows the calculated N_s dependence of the mass for an energy of $\omega_c/\omega_{LO} = 0.8$, from Ref. 15.

$\langle T \rangle_z$ represents the kinetic energy due to confinement in the direction perpendicular to the interface (z), and κ_2 is defined as before [Eq. (4)]. At fields above the quantum limit, the cyclotron-resonance transition occurs between the first and second Landau levels, and so E , the electron energy in the plane of the heterojunction, is set equal to the average energy of these levels, i.e., $E = \hbar\omega_c$.

Note that, in a heterojunction, $\langle T \rangle_z$ is not equivalent to the subband energy, and must be derived from the form of the wave function perpendicular to the interface. A suitable means of estimating $\langle T \rangle_z$ is to use the variational wave function of Fang and Howard:^{48,49}

$$\phi_0(z) = (\frac{1}{2}\beta^3)^{1/2} z e^{-\beta z/2}, \quad (6)$$

where $\beta^3 = 12m_0^*e^2(N_{\text{dep}} + 11N_s/32)/\epsilon\epsilon_0\hbar^2$, with N_{dep} equal to the depletion charge density. $\langle T \rangle_z$ is then obtained from the following expression:

$$\langle T \rangle_z = \frac{\hbar^2\beta^2}{8m_0^*}. \quad (7)$$

The depletion charges for the samples used in this study have previously been estimated to be $\sim 3 \times 10^{10} \text{ cm}^{-2}$ from measurements of the subband separation,⁴⁸ and this value was used to calculate $\langle T \rangle_z$; typical values obtained were $\sim 10 \text{ meV}$. Cyclotron-resonance measurements on bulk GaAs have revealed a low-energy cyclotron effective mass of $0.0660m_e$;^{3,41,42} this value includes the 3D polaron dressing, which can be removed by dividing by

$1 + \alpha/6$,²² where α is the Fröhlich coupling constant, to give a bulk-GaAs band-edge effective mass $m_0^* = 0.0652m_e$. κ_2 was again chosen to be -1.4 in order to represent the band nonparabolicity.^{3,41,48}

With the substitution of these parameters into Eq. (5) we have an estimate of the energy-dependent effective mass of the heterojunction electrons in the absence of polaron effects. Figure 7 shows the experimental effective masses for four different carrier densities, $N_s = 0.8 \times 10^{11} \text{ cm}^{-2}$, $1.4 \times 10^{11} \text{ cm}^{-2}$, $3.4 \times 10^{11} \text{ cm}^{-2}$, and $5.4 \times 10^{11} \text{ cm}^{-2}$, normalized using the masses $m_b^*(E)$ obtained from Eq. (5); in the absence of polaron effects, the normalized masses would be unity. With the energy dependence due to the band nonparabolicity removed, the size of the polaron contribution to the effective mass becomes very apparent; most notable is that the effective mass for $N_s = 5.4 \times 10^{11} \text{ cm}^{-2}$ is virtually unenhanced until very close to the LO-phonon energy, suggesting that the nonresonant part of the polaron effect is almost totally absent and that the resonant part is very small. As N_s decreases, both the nonresonant and resonant parts of the polaron contribution to the effective mass become larger. In order for a comparison with the limit of zero N_s to be made, normalized data for bulk GaAs (Refs. 3, 7, 42, and 44) are also shown in Fig. 7 as a dashed-dotted line (the same data as in Fig. 5): as the carrier densities in these samples are very low, the normalization has been carried out simply by setting $\langle T \rangle_z$ to zero in Eq. (5). At low energies ($< \sim 15 \text{ meV}$), where the enhancement of the effective mass is almost totally due to the nonresonant (i.e., energy-independent) part of the electron-LO-phonon interaction,²³ the heterojunction effective masses lie below the bulk data, but approach them as N_s tends to lower values. This is in satisfying agreement with the predictions of one-polaron theory, derived in the limit of low density and no screening, but including the finite width of the 2D EG,²³ which predicts a nonresonant part of the polaron effect which is the same in two and three

dimensions. Above the low-energy region ($> \sim 15 \text{ meV}$), the resonant-polaron enhancement of the heterojunction effective masses starts to become important at relatively high energies compared to the bulk data. However, as the LO-phonon energy is approached, the effective masses in the low-density heterojunctions start to increase more quickly than the bulk mass. By 33 meV , the total (resonant and nonresonant) polaron contribution to the effective mass in the heterojunction with $N_s = 1.4 \times 10^{11} \text{ cm}^{-2}$ appears to be enhanced over that in the bulk data, and to be increasing more rapidly with energy the data for the lower-carrier-density heterojunction with $N_s = 0.8 \times 10^{11} \text{ cm}^{-2}$ show an even steeper increase with energy. Thus, at energies close to the LO phonon, and for low 2D carrier densities, the resonant part of the polaron effect in GaAs-(Ga,Al)As heterojunctions appears to be enhanced over that in bulk GaAs. This is, again, in qualitative agreement with the one-polaron finite-width 2D EG theory,²³ although the functional form of the resonant contribution predicted differs from the experimental results.

In order to assess the factors contributing to the strong N_s dependence of the polaron effect, we must obviously turn to a more sophisticated theory. Polaron effects in GaAs-(Ga,Al)As heterojunctions have been extensively modeled using a memory-function approach, in which the shift in the cyclotron-resonance peak due to the polaron effect is calculated.^{15,16,23,47} This method calculates the memory function using second-order perturbation theory, treats the electrons and phonons as decoupled and includes only phonons at thermal equilibrium; the electron system can then be calculated within a variety of different approximations.¹⁶ It was found that the nonzero width of the 2D EG considerably reduces the polaron contribution to the cyclotron effective mass,^{15,23} by a factor of order 2 for $N_s = 4 \times 10^{11} \text{ cm}^{-2}$: the spatial extent of the lowest subband in the heterojunction decreases as N_s is raised,⁵⁰ and this should enhance the polaron effects. If the lowest Landau level is almost filled, the resonant part of the polaron effect will be suppressed, as the Pauli exclusion principle will reduce the number of final states for this virtual transition; the inclusion of the occupation probabilities of the Landau levels in the memory-function treatment⁴⁷ leads to a reduction of order 1.7 for $N_s = 10^{11} \text{ cm}^{-2}$ at $\omega_c/\omega_{\text{LO}} \sim 0.8$. The inclusion of static screening causes a further, but smaller reduction; interestingly, there is little difference between the effect of static and dynamic screening.¹⁶ The net result of these effects predicted by the calculations for GaAs-(Ga,Al)As heterojunctions was found to be a reduction of the polaron effect as N_s increases, the strongest N_s dependence of the suppression being due to the occupation effect.

In Fig. 7 we have plotted the results of these memory-function calculations¹⁶ including occupation effects, dynamic screening and the finite thickness of the 2D EG, as a solid line. The theoretical curve, which was derived for $N_s = 4 \times 10^{11} \text{ cm}^{-2}$, and which thus should lie between the experimental results for $N_s = 3.4 \times 10^{11}$ and $5.4 \times 10^{11} \text{ cm}^{-2}$ seems to overestimate the polaron contribution to the effective mass between 25 and 32 meV , but lies between the experimental results closer to the LO-phonon

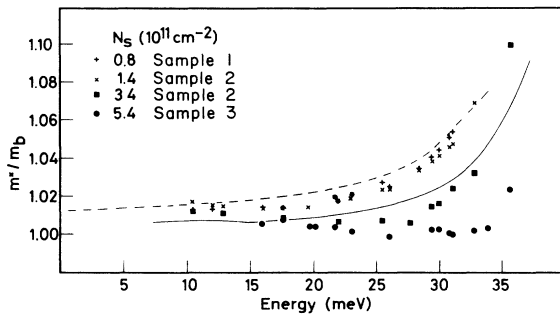


FIG. 7. The normalized effective mass m^*/m_b^* as a function of energy for four different 2D electron concentrations. The experimental data, shown as points, are normalized using the procedure to remove band nonparabolicity described in the text. Low-energy data for $N_s = 5.4 \times 10^{11} \text{ cm}^{-2}$ have been omitted for clarity. Normalized bulk GaAs data are shown as a dashed-dotted line for comparison (the same data as in Fig. 5). The theoretical predictions of the memory-function model¹⁶ for $N_s = 4.0 \times 10^{11} \text{ cm}^{-2}$ are shown as a solid line.

crucial role in the magnetophonon effect;⁵¹ without broadening the magnetophonon-resonance peaks in two dimensions will be δ -function singularities, whereas in three dimensions only a logarithmic divergence occurs. In two dimensions the effect of the broadening is to very slightly shift the magnetophonon resonances in ρ_{xx} to lower fields than expected from the resonance condition;⁵¹ although the shifts are far too small, this is perhaps a qualitative explanation for the apparent down-shifted phonon frequency observed by Brummell *et al.*,¹⁷ which was deduced from the fact that the MPR peaks were at a slightly lower field than those for bulk GaAs. Another point is that the magnetophonon results are taken at high temperatures, where the polaron coupling has been shown to be modified.¹⁷ It has recently been shown that the magnetophonon-resonance fields can be very strongly carrier-concentration dependent,⁵² and this may be related to the N_s -dependent coupling shown here. Finally, it must be remarked that resonant-polaron cyclotron resonance provides a very direct way in which to observe the phonon involved in the polaron effect; the derivation of a phonon frequency from MPR is a considerably more involved process.¹⁷

V. SUMMARY

The cyclotron resonance of two-dimensional electrons in several GaAs-(Ga,Al)As heterojunctions has been studied in reflectivity up to an energy of 35.63 meV, close to the GaAs longitudinal-optical-phonon energy (36.7

meV), enabling the energy of the resonant-polaron condition to be accurately deduced. A calculation of the dielectric response of the heterojunctions was used to reproduce the observed CR line shapes well, enabling the effective mass to be reliably evaluated. It was found that the resonant-polaron effect occurs at the LO-phonon energy, in agreement with theoretical predictions, and in contrast to the recent interpretations of magnetophonon-resonance measurements. However, the strength of the effect observed both in the CR linewidth and the value of the effective mass is a strong function of the 2D carrier density (N_s), indicating the importance of occupation effects and screening. For $N_s > 5 \times 10^{11} \text{ cm}^{-2}$ both the nonresonant and resonant polaron effects are very small. The strong N_s dependence explains previous conflicting reports in the literature of "enhanced" or "reduced" polaron effects in the 2D electron gas.

ACKNOWLEDGMENTS

We should like to thank A. F. van Etteger, K. van Hulst, T. J. B. M. Janssen, H. van Luong, and J. Rook for invaluable technical support. Part of this work was supported by the "Stichting voor Fundamenteel Onderzoek der Materie" (FOM), with financial support from the "Nederlandse Organisatie voor Wetenschappelijk Onderzoek" (NWO) (Netherlands), and by the Science and Engineering Research Council (SERC) of Great Britain.

*Present address: Centre National de la Recherche Scientifique/Service National des Champs Intenses, 25 Avenue des Martyrs, Boîte Postale 166X, F-38042 Grenoble Cédex, France.

¹P. Pfeffer and W. Zawadzki, *Solid State Commun.* **57**, 847 (1986); *Phys. Rev. B* **37**, 2695 (1988).

²H. Sigg, H. J. A. Bluyssen, and P. Wyder, *Solid State Commun.* **48**, 897 (1983).

³M. A. Hopkins, R. J. Nicholas, P. Pfeffer, W. Zawadzki, D. Gauthier, J. C. Portal, and M. A. DiForte-Poisson, *Semicond. Sci. Technol.* **2**, 568 (1987).

⁴S. Das Sarma, *Phys. Rev. Lett.* **52**, 859 (1984).

⁵D. M. Larsen, *Phys. Rev. B* **30**, 4807 (1984).

⁶Wu Xiaoguang, F. M. Peeters, and J. T. Devreese, *Phys. Status Solidi B* **133**, 229 (1986).

⁷H. Sigg, P. Wyder, and J. A. A. J. Perenboom, *Phys. Rev. B* **31**, 5253 (1985).

⁸J. Singleton, R. J. Nicholas, and F. Nasir, *Solid State Commun.* **58**, 833 (1986).

⁹M. Horst, U. Merkt, W. Zawadzki, J. C. Maan, and K. Ploog, *Solid State Commun.* **53**, 403 (1985).

¹⁰M. A. Hopkins, R. J. Nicholas, M. A. Brummell, J. J. Harris, and C. T. Foxon, *Superlatt. Microstruct.* **2**, 319 (1986).

¹¹M. Ziesmann, D. Heitmann, and L. L. Chang, *Phys. Rev. B* **35**, 4541 (1987).

¹²J. Singleton, R. J. Nicholas, D. C. Rogers, and C. T. B. Foxon, *Surf. Sci.* **196**, 429 (1988).

¹³M. Horst, U. Merkt, and J. P. Kotthaus, *Phys. Rev. Lett.* **50**, 754 (1983).

¹⁴R. Lassnig and W. Zawadzki, *Surf. Sci.* **142**, 388 (1984).

¹⁵Wu Xiaoguang, F. M. Peeters, and J. T. Devreese, *Phys. Rev. B* **34**, 8800 (1986).

¹⁶F. M. Peeters, Wu Xiaoguang, and J. T. Devreese, *Surf. Sci.* **196**, 437 (1988).

¹⁷M. A. Brummell, R. J. Nicholas, M. A. Hopkins, J. J. Harris, and C. T. Foxon, *Phys. Rev. Lett.* **58**, 77 (1987).

¹⁸Wu Xiaoguang, F. M. Peeters, and J. T. Devreese, *Phys. Rev. B* **36**, 9765 (1987).

¹⁹Marcos H. Degani and Oscar Hipolito, *Phys. Rev. Lett.* **59**, 2820 (1987).

²⁰R. J. Nicholas, L. C. Brunel, S. Huant, K. Karraï, J. C. Portal, M. A. Brummell, M. Razeghi, K. Y. Cheng, and A. Y. Cho, *Phys. Rev. Lett.* **55**, 883 (1985).

²¹L. C. Brunel, S. Huant, R. J. Nicholas, M. A. Hopkins, M. A. Brummell, K. Karraï, J. C. Portal, M. Razeghi, K. Y. Chen, and A. Y. Cho, *Surf. Sci.* **170**, 542 (1986).

²²P. G. Harper, J. W. Hodby, and R. A. Stradling, *Rep. Prog. Phys.* **36**, 1 (1973).

²³F. M. Peeters, Wu Xiaoguang, and J. T. Devreese, *Phys. Scr.* **T 13**, 282 (1986).

²⁴C. T. Foxon, J. J. Harris, R. G. Wheeler, and D. E. Lacklison, *J. Vac. Sci. Technol. B* **4**, 511 (1986).

²⁵H. Sigg, H. J. A. Bluyssen, and P. Wyder, *IEEE J. Quantum Electron.* **QE-20**, 616 (1984).

²⁶G. Abstreiter, J. P. Kotthaus, J. F. Koch, and G. Dorda, *Phys. Rev. B* **14**, 2840 (1976).

²⁷G. L. J. A. Rikken, H. Sigg, C. J. G. M. Langerak, H. W. Myron, and J. A. A. J. Perenboom, *Phys. Rev. B* **34**, 5590 (1986).

- (1986).
- ²⁸Z. Schlesinger, J. C. M. Hwang, and S. J. Allen, *Phys. Rev. Lett.* **50**, 2098 (1983).
- ²⁹K. Karrai, S. Huant, G. Martinez, and L. C. Brunel, *Solid State Commun.* **66**, 355 (1988).
- ³⁰K. A. Maslin, T. J. Parker, N. Raj, D. R. Tilley, P. J. Dobson, D. Hilton, and C. T. Foxon, *Solid State Commun.* **60**, 461 (1987).
- ³¹M. von Ortenburg, *Solid State Commun.* **17**, 1335 (1975).
- ³²M. A. Hopkins, R. J. Nicholas, D. J. Barnes, C. T. Foxon, and J. J. Harris (unpublished).
- ³³K. W. Chiu, T. K. Lee, and J. J. Quinn, *Surf. Sci.* **58**, 182 (1976).
- ³⁴T. A. Kennedy, R. J. Wagner, B. D. McCombe, and J. J. Quinn, *Solid State Commun.* **18**, 275 (1976).
- ³⁵Z. Schlesinger, W. I. Wang, and A. H. MacDonald, *Phys. Rev. Lett.* **58**, 73 (1987).
- ³⁶D. Heitmann, M. Ziesmann, and L. L. Chang, *Phys. Rev. B* **34**, 7463 (1986).
- ³⁷K. Ensslin, D. Heitmann, H. Sigg, and K. Ploog, *Phys. Rev. B* **36**, 8177 (1987).
- ³⁸R. J. Nicholas, P. J. van der Wel, and J. Singleton (unpublished).
- ³⁹J. Singleton, R. J. Nicholas, N. J. Pulsford, N. R. Couch, and M. J. Kelley, *J. Phys. (Paris) Colloq.* **48**, C5-435 (1987).
- ⁴⁰E. D. Palik, G. S. Picus, S. Teitler, and R. F. Wallis, *Phys. Rev.* **122**, 475 (1961).
- ⁴¹W. Zawadzki and P. Pfeffer, in *High Magnetic Fields in Semiconductor Physics*, Vol. 71 of *Springer Series in Solid-State Sciences*, edited by G. Landwehr (Springer, Berlin, 1987), p. 523.
- ⁴²H. Sigg, J. A. A. J. Perenboom, P. Pfeffer, and W. Zawadzki, *Solid State Commun.* **61**, 685 (1987).
- ⁴³M. Braun and U. Rössler, *J. Phys. C*: **18**, 3365 (1985).
- ⁴⁴J. A. A. J. Perenboom and H. Sigg (unpublished); M. A. Hopkins and R. J. Nicholas (unpublished).
- ⁴⁵G. L. J. A. Rikken, H. W. Myron, C. J. G. M. Langerak, and H. Sigg, *Surf. Sci.* **170**, 160 (1986).
- ⁴⁶M. A. Brummell, D. R. Leadley, R. J. Nicholas, J. J. Harris, and C. T. Foxon, *Surf. Sci.* **196**, 451 (1988).
- ⁴⁷Wu Xiaoguang, F. M. Peeters, and J. T. Devreese, in *Proceedings of the 18th International Conference on the Physics of Semiconductors*, edited by O. Engström (World Scientific, Singapore, 1987), p. 589.
- ⁴⁸M. A. Hopkins, R. J. Nicholas, M. A. Brummell, J. J. Harris, and C. T. Foxon, *Phys. Rev. B* **36**, 4789 (1987).
- ⁴⁹F. F. Fang and W. E. Howard, *Phys. Rev. Lett.* **16**, 797 (1966).
- ⁵⁰F. Stern and W. E. Howard, *Phys. Rev.* **163**, 816 (1967).
- ⁵¹P. Warmenbol, F. M. Peeters, and J. T. Devreese, *Phys. Rev. B* **37**, 4694 (1988).
- ⁵²D. R. Leadley, R. J. Nicholas, M. S. Skolnick, S. J. Bass, and L. L. Taylor, in *Proceedings of the International Conference on the Application of High Magnetic Fields in Semiconductor Physics, Würzburg, 1988*, edited by G. Landwehr (Springer, Berlin, in press).